RESULTS OF NASA'S FIRST AUTONOMOUS FORMATION FLYING EXPERIMENT: EARTH OBSERVING-1 (EO-1)

David Folta[+]
NASA/Goddard Space Flight Center
Greenbelt, MD

Albin Hawkins[#]
a.i.-solutions, Inc.
Lanham, MD

ABSTRACT

NASA's first autonomous formation flying mission completed its primary goal of demonstrating an advanced technology called enhanced formation flying. To enable this technology, the Guidance, Navigation, and Control center at the Goddard Space Flight Center implemented a universal 3-axis formation flying algorithm in an autonomous executive flight code onboard the New Millennium Program's (NMP) Earth Observing-1 (EO-1) spacecraft. This paper describes the mathematical background of the autonomous formation flying algorithm and the onboard flight design and presents the validation results of this unique system. Results from functionality assessment through fully autonomous maneuver control are presented as comparisons between the onboard EO-1 operational autonomous control system called AutoCon™, its ground-based predecessor, and a standalone algorithm.

INTRODUCTION

The need for an innovative technical approach to autonomously achieve and maintain formations of spacecraft is essential as scientific objectives become more ambitious.[1,2] The development of small low-cost spacecraft and new scientific research such as large scale interferometry has led many programs to recognize the advantage of flying multiple spacecraft in formation to achieve correlated instrument measurements. Advances in automation and technology by the Guidance Navigation and Control (GN&C) center at the Goddard Space Flight Center (GSFC) have resulted in the development and demonstration of an autonomous system to meet these new guidelines. The EO-1 NMP technology called Enhanced Formation Flying (EFF) incorporates the Folta-Quinn three-axis universal algorithm for formation control into this advanced system.[3] This system can be used by single spacecraft for orbit maintenance or by spacecraft in constellations and formations as shown in Figure 1. It can also be applied to low Earth orbits, highly elliptical orbits, and non-Keplerian trajectories such as libration orbits. The technology allows the burden

Figure 1. EO-1 Formation Flying Behind Landsat-7

+. Aerospace Engineer, NASA GSFC, Guidance, Navigation, and Control Center, Greenbelt, Md. Senior member AIAA
#. Senior Systems Engineer, a.i.-solutions, Inc. Lanham, Md

in maneuver planning and execution to be placed onboard the spacecraft, mitigating some of the associated operational concerns while increasing autonomy.

The EO-1 formation flying technology requirements are: to demonstrate the capability of EO-1 to autonomously fly over the same groundtrack as Landsat-7 within +/-3 kilometers at the equator, autonomously maintain the formation for extended periods to enable paired scene comparisons between the two satellites, and to provide an onboard system to transfer commands, telemetry, and serve as the executive. The required relative separation is 1 minute in mean motion, equivalent to 450km alongtrack at the circular mission altitude of 705km. The tolerance on this separation to meet the +/-3 kilometer ground track is approximately +/- 6 seconds, or roughly 75 km.

This paper presents validation results of formation flying of the NMP EO-1 spacecraft with respect to the Landsat-7 spacecraft. Results are presented as maneuver comparisons between the onboard autonomous formation flying control system and ground systems. Both the onboard and the prime ground systems use AutoCon™, a high fidelity modeling package that incorporates the Folta-Quinn algorithm. A comparison is also made to the original design in MATLAB™ and the change to orbital parameters by the EO-1 formation flying maneuvers as reflected in the orbit determination solutions.

FORMATION FLYING

Formation flying involves position maintenance of multiple spacecraft relative to measured separations. For EO-1, this relative separation between the EO-1 and Landsat-7 spacecraft is required to allow co-scene comparisons. An overview of the EO-1 formation flying using a two spacecraft differential drag example is presented here.

Mechanics Using Differential Drag

If two spacecraft are placed in similar orbital planes and similar altitudes with a small initial anomaly separation angle they will be equally affected by the potential field of the Earth and by atmospheric drag provided that they have identical ballistic properties. As long as the separation angle is small enough that atmospheric density and gravitational perturbations can be considered constant, the relative separation will remain the same. If the spacecraft are separated in the radial direction, their orbit velocities are different, and one spacecraft (the EO-1 / chase spacecraft) will appear to drift relative to the other (Landsat-7 / control spacecraft). The drifting is most apparent in the along-track (orbital velocity) direction. The initial radial separation can be operationally planned by taking into account the respective ballistic properties of each spacecraft or induced by differential decay rates caused by environmental perturbations. The concept of formation flying for EO-1 is based on the constructive use of the differential decay rates as a direct function of differential ballistic properties between a control and a chase spacecraft.

EO-1 Example

An example of the orbit dynamics of EO-1 and Landsat-7 formation flying is shown in Figure 2. In the figure, EO-1 starts in formation at the red dot location, behind Landsat-7 by 450 kilometers and above by ~50 meters. Due to the differences in the atmosphere drag accelerations, the EO-1 orbit decays slightly faster. While in a higher orbit than Landsat-7, EO-1 is drifting away from Landsat-7 since the average orbital velocity is less. After several days of orbital decay due to

atmospheric drag, EO-1 will be below Landsat-7 and will drift towards it since the average orbital velocity is now higher. When EO-1 is outside the required tolerance box or if Landsat-7 has maneuvered, EO-1 will autonomously compute and perform a maneuver to reposition it to an initial condition to repeat the relative motion.

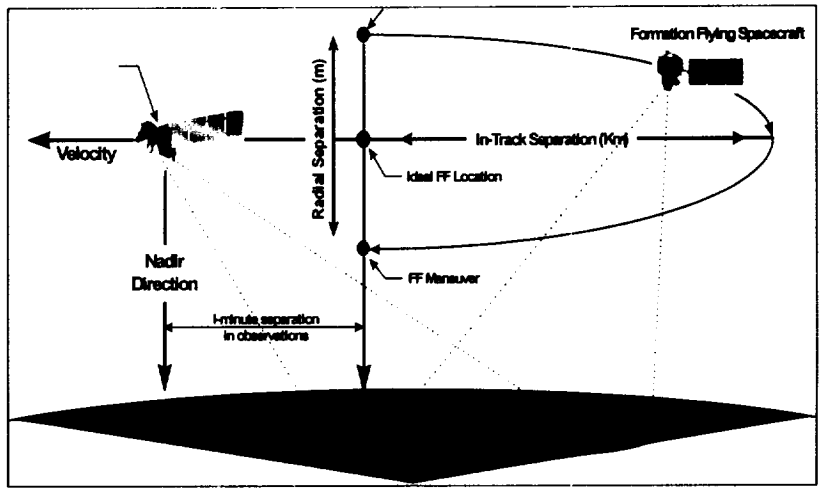

Figure 2. EO-1 Formation Flying Using Differential Drag

FORMATION FLYING ALGORITHM

The Folta-Quinn (FQ) algorithm is a new technology that is based on mathematics derived by Battin and adapted to the formation flying problem.[3,4,5] This technology allows full closed-loop maneuver autonomy onboard any spacecraft rather than the tedious and costly operational activity historically associated with ground based operations and control.

FQ Algorithm Description

The FQ algorithm for formation flying solves the position maintenance problem by combining a modified Lambert's two point boundary value problem and Battin's 'C*' matrix with an autonomous system developed by a.i. solutions, Inc. of Lanham, MD called AutoCon™.[6] The algorithm enables the spacecraft to autonomously execute complex three-axis orbital maneuvers. Figure 3 illustrates the basic sets of information required for the EO-1 formation targeting as it is incorporated into AutoCon™. The FQ algorithm well is suited for multiple three-axis burn scenarios but is more easily explained using a two-burn, co-planar example for clarity.

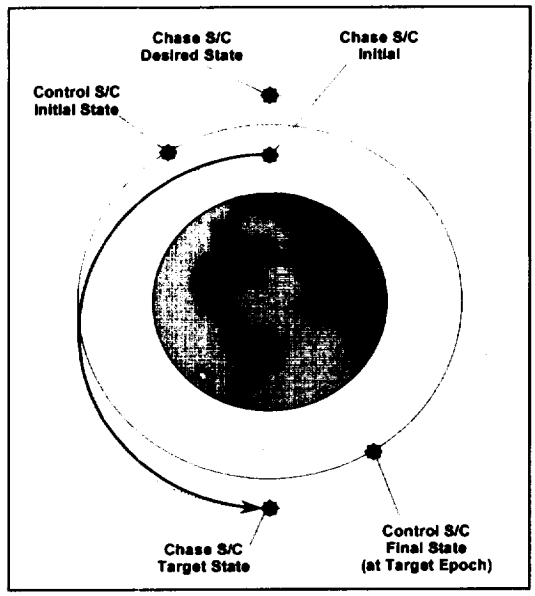

Figure 3. FQ Algorithm Inputs for EO-1 Formation Flying

The formation flying problem in this example involves two spacecraft orbiting the Earth. Landsat-7, the control spacecraft, orbits without performing any formation flying maneuvers. EO-1, the chase spacecraft monitors the control spacecraft, and performs maneuvers designed to maintain the relative position imposed by the formation requirements. In this example, the goal of the formation flying algorithm is for EO-1 to perform maneuvers which cause it to move along a specific transfer orbit. The transfer orbit is established by determining a path (in this case a Keplerian path) which will carry the EO-1 spacecraft from some initial state, ($\mathbf{r}_0$, $\mathbf{v}_0$), at a given time, t_0, to a target state, ($\mathbf{r}_t$, $\mathbf{v}_t$), at a later time, t_t. The target state is found to be one which will place EO-1 in a location relative to Landsat-7 so as to maintain the formation. A desired state is also computed. This is accomplished by back propagating the target state to find the initial state that EO-1 would need at time t_0 for it to achieve the target state at time t_t without executing a maneuver. This back propagation of the target state gives rise to the desired state, ($\mathbf{r}_d$, $\mathbf{v}_d$) at time t_0. The initial state can now be differenced from the desired state to find:

$$\begin{pmatrix} \delta r \\ \delta v \end{pmatrix} = \begin{pmatrix} r_0 - r_d \\ v_0 - v_d \end{pmatrix}$$

STM Formulation

The FQ Algorithm uses state transition matrices, described below, for the calculation of the maneuver ΔV. Selecting initial conditions prescribed at a time t_0 so that the state at this time has all zero components except the jth term which is unity, a state transition matrix, $\Phi(t_1,t_0)$, can be constructed such that it will be a function of both t and t_0 and satisfies matrix differential equation relationships[5]. The initial conditions of $\Phi(t_1,t_0)$ are the identity matrix.

Having partitioned the state transition matrix, $\Phi(t_1,t_0)$ for time $t_0 < t_1$,

$$\phi(t_1,t_0) \equiv \begin{bmatrix} \phi_1(t_1,t_0)\phi_2(t_1,t_0) \\ \phi_3(t_1,t_0)\phi_4(t_1,t_0) \end{bmatrix}$$

We find the inverse may be directly obtained by employing symplectic properties

$$\phi^{-1}(t_1,t_0) \equiv \phi(t_0,t_1) \equiv \begin{bmatrix} \phi_1(t_0,t_1)\phi_2(t_0,t_1) \\ \phi_3(t_0,t_1)\phi_4(t_0,t_1) \end{bmatrix}$$

$$\phi^{-1}(t_1,t_0) \equiv \begin{bmatrix} \phi^T{}_4(t_1,t_0)\phi^T{}_2(t_1,t_0) \\ \phi^T{}_3(t_1,t_0)\phi^T{}_1(t_1,t_0) \end{bmatrix}$$

Where the matrix $\Phi(t_0,t_1)$ is based on a propagation forward in time from t_0 to t_1 and is sometimes referred to as the navigation matrix, and $\Phi(t_1,t_0)$ is based on a propagation backward in time from t_1 to t_0, and is sometimes referred to as the guidance matrix. We can further define the transition matrix partitions as follows:

$$\tilde{R}^*(t_0) \equiv \phi_1(t_0,t_1) \quad \tilde{R}\ (t_1) \equiv \phi_1(t_1,t_0)$$
$$R^*(t_0) \equiv \phi_2(t_0,t_1) \quad R\ (t_1) \equiv \phi_2(t_1,t_0)$$
$$\tilde{V}^*(t_0) \equiv \phi_3(t_0,t_1) \quad \tilde{V}\ (t_1) \equiv \phi_3(t_1,t_0)$$
$$V^*(t_0) \equiv \phi_4(t_0,t_1) \quad V\ (t_1) \equiv \phi_4(t_1,t_0)$$

Substituting yields the following useful identities:

$$\begin{bmatrix} \tilde{R}^*(t_0) & R^*(t_0) \\ \tilde{V}^*(t_0) & V^*(t_0) \end{bmatrix} = \begin{bmatrix} V^T(t_1) & -R\ (t_1) \\ -\tilde{V}^T(t_1) & \tilde{R}\ (t_1) \end{bmatrix}$$

Where the starred quantities are based upon a guidance matrix and unstarred quantities are based on a navigation matrix. If a reversible Keplerian path is assumed between the two states, one should expect the forward projection of the state from t_0 to t_1 to be related to the backward projection of the state from t_1 to t_0. When the fundamental matrices $\tilde{C}^*$ and C^* are defined as

$$\tilde{C}^* \equiv \tilde{V}^* \tilde{R}^{*-1} \text{ and } C^* \equiv V^* R^{*-1}$$

We find the following:

$$\tilde{C}^* \equiv \left.\frac{\partial v_0}{\partial r_0}\right|_{v1=cons\tan t} \text{ and } C^* \equiv \left.\frac{\partial v_0}{\partial r_0}\right|_{r1=cons\tan t}$$

so that $C^*\delta r = \delta v_0$ becomes the velocity deviation required at time t_0 as a function of the measured position error δr at time t_0 if the spacecraft is to arrive at the reference position r_1 at time t_1 (with arbitrary velocity). Recalling that the starred quantities were obtained based on the guidance matrix, the sympletic property allows them to be computed based on a navigation projection. It can therefore be shown that

$$\left[C^*(t_0)\right] = \left[V^*(t_0)\right]\left[R^*(t_0)\right]^{-1} = \left[\tilde{R}^T(t_1)\right]\left[-R^T(t_1)\right]^{-1}$$

Applying a universal variable formulation of the closed-form state transition matrix, the relevant state transition matrix submatrices are computed.[4,5] The expressions for F, G, F_t and G_t are derived from the Gauss problem of planar motion; K is a quantity derived from the Universal Variable (U) formulation.[5] These variables are dependent upon each other in their formulation, i.e. U(6) is dependent upon U(4) and on intermediate variables related to the classic f and g series. The target and desired states, r_d ,v_d, r_t , and v_t are computed from the propagated states. μ is the universal gravitational constant. R and $\tilde{R}$ are then defined from the target and desired states as:

$$\mathbf{R}(t_f) = \frac{|\mathbf{r}_d|}{\mu}(1-F)\left[(\mathbf{r}_t - \mathbf{r}_d)\mathbf{v}_d^T - (\mathbf{v}_t - \mathbf{v}_d)\mathbf{r}_d^T\right] + \frac{K}{\mu}\left[\mathbf{v}_t\mathbf{v}_d^T\right] + G\left[\mathbf{I}\right]$$

$$\tilde{\mathbf{R}}(t_f) = \frac{|\mathbf{r}_t|}{\mu}\left[(\mathbf{v}_t - \mathbf{v}_d)(\mathbf{v}_t - \mathbf{v}_d)^T\right] + \frac{1}{|\mathbf{r}_t^3|}\left[\mathbf{r}_t|(1-F)\mathbf{r}_t\mathbf{r}_d^T + K\mathbf{v}_t\mathbf{r}_d^T\right] + F\left[\mathbf{I}\right]$$

From these variables and sub-matrices, the C* matrix is computed as follows:

$$R^*(t_0) = -R^T(t_t)$$
$$V^*(t_0) = \tilde{R}^T(t_t)$$
$$C^*(t_0) = V^*(t_0)\left[R^*(t_0)\right]^{-1}$$

The expression for the impulsive maneuver follows immediately:

$$\Delta V = \left[C^*(t_0)\right]\delta r_0 - \delta v_0$$

At each step in the process, the next control point on the reference path can be examined and back-propagated along a Keplerian path to determine small differences between spacecraft position and velocity on the reference path and determine which Keplerian path would intersect the reference path at the next control point. These differences are then fed into the propagator via the state transition matrices to determine the incremental ΔV required to get the spacecraft to the next control position on the reference trajectory. At the conclusion of the maneuver window, a final burn is required to match the velocity needed to maintain the new Keplerian trajectory. One can use single or multiple maneuvers to achieve the target condition. For EO-1's orbit a long, iterative window requiring many small burns is not necessary and ΔV maneuvers resemble a Hohmann transfer.

Formation Flying Control

The AutoCon™ flight control system ingest data from EO-1 sensors and subsystems such as propulsion, navigation, and attitude data.[6] It then autonomously generates, analyzes, and executes the maneuvers required to initialize and maintain the formation between Landsat-7 and EO-1. Because these calculations and decisions are performed onboard the spacecraft, the lengthy period of ground-based planning previously required prior to maneuver execution is eliminated. The system is general and modular so that it can be easily extended to future missions. Furthermore, the AutoCon™ flight control system is designed to be compatible with various onboard navigation systems (i.e. GPS, or an uploaded ground-based ephemeris). The AutoCon™ system is embedded in the Mongoose-5 EO-1 spacecraft computer. Interfaces are handled with one interface to the C&DH system. This is used for the ingest of GPS state information, AutoCon™ commanding, telemetry, and maneuver commands for EO-1 as well. The FQ algorithm needs input data for the current EO-1 state, the target state, and the desired state. These data are provided by AutoCon™. AutoCon™ takes the current EO-1 and uploaded Landsat-7 states and then propagates these states for a user-specified fraction of the orbit period. Autonomous orbit control of a single spacecraft requires that a known control regime be established by the ground which is consistent with mission parameters. That data must then be provided to the spacecraft. When orbital perturbations carry the spacecraft close to any of the established boundaries, the spacecraft reacts (via maneuver) to maintain itself within its error box. The EO-1 system is currently set to check the tolerance requirements every 12 hours. From this point AutoCon™ propagates the states for 48 hours (a commandable setting) and will execute a maneuver plan if needed.

Algorithm Modes for Validation

There are five EFF maneuver control modes onboard EO-1 as shown in Figure 4. All control modes were verified during the onboard validation process. These modes were established to allow an incremental validation of the system performance, data interfaces, and maneuver computations before commands were generated onboard for an executable maneuver. Modes 1 and 2 were validated in functional tests while modes 3-5 were validated as executed EO-1 maneuvers.

ΔV Computations and Quantized Maneuvers

The computation of the EO-1 maneuver ΔVs is performed using a sequence of two methods. The first method uses the FQ algorithm for the calculation of the maneuver to reach the targeted position relative to Landsat-7. Subsequently, a simple velocity-matching maneuver is then performed once the targeted position is attained. The FQ algorithm could also be used, but in an effort to simplify onboard processes, as no state propagation is necessary, a velocity matching method is employed. This velocity matching is computed from the predicted difference in the velocity of the EO-1 transfer orbit and the targeted state at the target position.

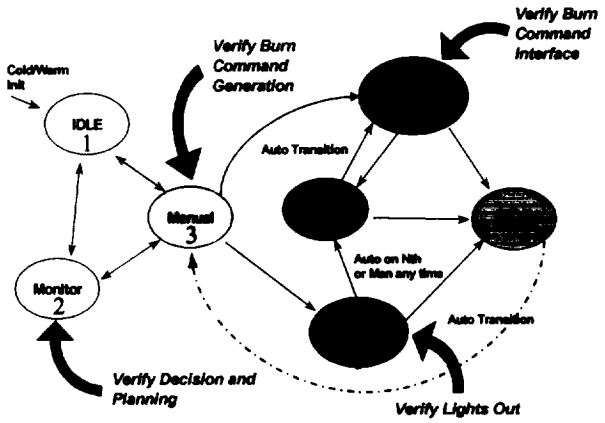

Figure 4 EFF Maneuver Modes

The EO-1 spacecraft propulsion system was designed so that the minimum maneuver duration is one second with larger burns selectable at one-second increments. This means that commands generated either onboard or on the ground will undergo a rounding of the maneuver duration based on the computed ΔV. For example if a maneuver is such that the computed maneuver duration is 5.49 seconds, the commanded maneuver will actually be 5 seconds, and a 5.51 second duration would become 6 seconds. This results in a quantized maneuver duration for each maneuver and thus the achieved Keplerian trajectory will differ slightly from the targeted trajectory. To compensate for this effect the final ΔV is adjusted. The velocity match is perturbed slightly to compensate for the position error resulting from the prior maneuver's quantized burn duration. This allows the targeted orbit's sma to be achieved with a trivial sacrifice of eccentricity.

VALIDATION AND PERIOD OF PERFORMANCE

On January 12, 2001, the EFF experiment onboard EO-1 became operational. Validation scripts ran over a several month period, January 12th through June 28th 2001 and generated over 600 maneuver plans. In the time period of April to June, eight maneuver commands were generated onboard as operational maneuvers to control the formation. The validation tests were divided into two areas: functional test of modes 1 and 2, and autonomous maneuver execution tests of modes 3, 4, and 5.

Validation process

EFF was initially validated in modes 1 and 2 whereby GPS states and data required for the onboard process flowed though the C&DH interface into the AutoCon™ executable and appraisal maneuvers were then computed. Manual and semi-autonomous modes were then used over a period of two months to validate against maneuvers computed by the flight operations team. Finally, fully autonomous maneuvers were successfully planned and executed. Scripts and data required for these planning cycles were placed onboard via tables uploads whenever necessary. The overall computational interval varied according to the mode, as mode 2 functional tests were run continuously for six weeks taking approximately 3 hours in duration for each GPS ingested state while fully autonomous test took only an hour. The manual, semi-autonomous, and fully-autonomous maneuver modes used either a ground based S-band derived state or an onboard GPS state.

Functional Tests

The GPS state, along with an uploaded Landsat-7 state, was then propagated onboard for durations of 12 hours, 24 hours, and 48 hours in the functional tests. Maneuvers were computed at 12, 24, and 48 hour epoch marks past the GPS ingested state epoch. These tests enabled the computation of maneuvers while verifying data ingest and related data interfaces, propagation of states, and generation of maneuver commands (maneuver duration and an attitude quaternion) onboard EO-1. Functional maneuver tests were planned in sets of three based on the three aforementioned propagation durations. GPS data was ingested 177 times while tables were uploaded approximately 30 times for script control, Landsat-7 data, and environmental data updates. The functional validation was accomplished by comparing several events and computations[7]. These tests included:

- EO-1 GPS and Landsat-7 state ingest
- EO-1 and Landsat-7 Propagation Events (Generate Target and Desired States)
- Folta-Quinn Targeting Algorithm Output
  - quantized maneuver ΔV
  - three-axis maneuver ΔV
  - internal calculations (matrices, variables, states)

Autonomous Tests

The autonomous maneuver execution tests were accomplished less frequently as they were tied to the operational maneuver timeline but were computed in much the same manner as the functional continuous tests with the following exceptions. The onboard maneuvers were planned with either a ground based S-band definitive orbit determination solution or the output of the GPS system onboard EO-1. This state along with an uploaded Landsat-7 state was propagated onboard for either 1 hour or 13 hours depending on input state epoch. Maneuvers were planned at a required maneuver epoch with the output used for planning of EO-1 formation flying maintenance maneuvers. The command data was passed though the C&DH system for inclusion into the absolute time sequence just as if the command had been generated on the ground. The radial target varied over the demonstration as the atmospheric density was changing and the relative decay rates of both spacecraft needed to be considered. The radial target relative to Landsat-7 varied over 20m, 40, 50, or 60m in order to yield a predicted relative motion profile.

Maneuver Comparisons

This section presents results of the comparison between onboard and ground in terms of the absolute difference in the computed ΔV and the related percentage error for several maneuver scenarios. The results for functional and maneuver tests are further divided by whether they are quantized or total three-axis computations as the maneuvers executed onboard for formation maintenance used only quantized ΔVs and durations derived from the total three-axis ΔV computation.

Functional Validation

A total of 12 scenarios consisting of 3 maneuver sets (two maneuvers per set) for a total of 36 combined maneuvers were selected for functional validation. The locations and epochs of these maneuvers were chosen randomly at approximately one per day over a three-week span. Figure 5 presents the overall performance of each quantized maneuver as an absolute percentage difference in the ΔV magnitude. The mean value of the quantized maneuver difference is 0.0001890cm/s with a standard deviation of 0.000133 cm/s. These data show that there is excellent functional agreement between the onboard system and ground validation system. The larger residual in figure 5 is due to a 1-second quantization of a velocity-matching maneuver. This difference is due to the onboard system yielding a maneuver duration near the mid point which rounded down while the ground system rounded up. This difference is still small at 1.4%.

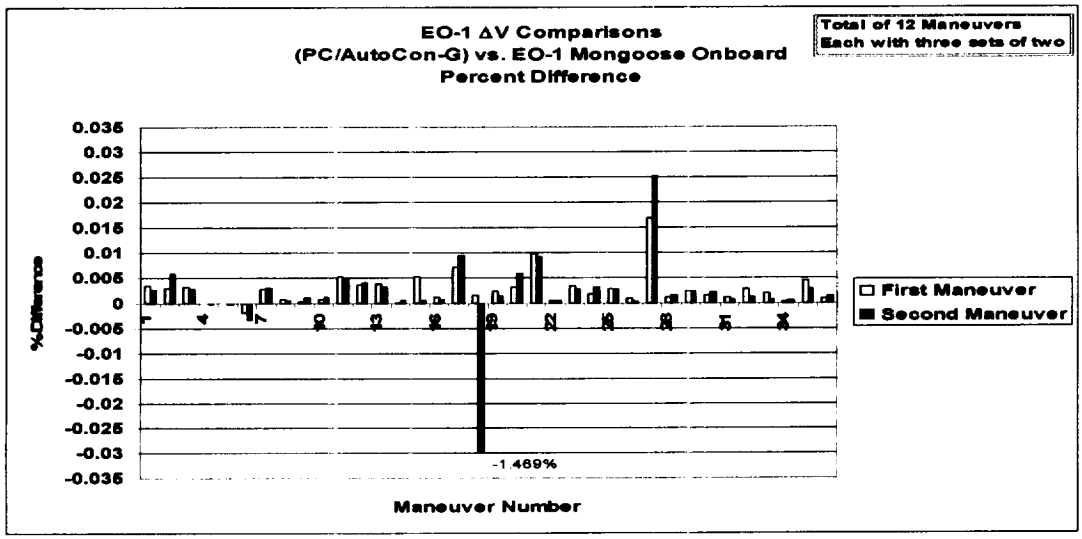

Figure 5. Percentage Difference in EO-1 Onboard and Ground Absolute ΔVs

Figure 6 presents maneuver comparisons for the ground vs. onboard three-axis computation. This provides the comparisons for the total ΔV required to align EO-1 directly behind Landsat-7 and involves all three ΔV components of radial, alongtrack, and crosstrack. The ΔVs ranged from 1cm/s to 1.2m/s for the quantized maneuvers and from 1.6m/s to 133m/s for the three-axis computation. The quantized maneuvers are the ΔVs that are applied to the EO-1 formation maintenance to accommodate the one-minute separation and the Earth's rotation in one minute to

meet the 3km ground track requirement. The comparisons show only the total ΔV magnitude, as this is the only information available in EO-1 playback telemetry.

With the comparisons between the ground and operational onboard version of the EFF completed, a comparison to the original FQ algorithm code was then performed. This comparison was done only for the first FQ targeted maneuver of each maneuver scenario. The state data from the playback telemetry was input into a MATLAB™ script with the FQ algorithm computing the maneuver without any propagation.[3, 8] Figure 7 shows the difference as a percentage respectively for the three-axis ΔV and an alongtrack ΔV. The alongtrack ΔV was represented in the MATLAB™ script by using a local-vertical local horizontal coordinate system based on the input state in a manner which is comparable to the EO-1 nominal attitude for maneuvers. The resulting ΔV difference gives a mean of 0.0727 cm/s and a standard deviation of 0.348058 cm/s for the three-axis and gives a mean of -0.03997 cm/s and a standard deviation of 0.278402 cm/s for the alongtrack. The mean percentage difference was 0.003 for the three-axis and 0.006 for the alongtrack. These results show excellent comparisons.

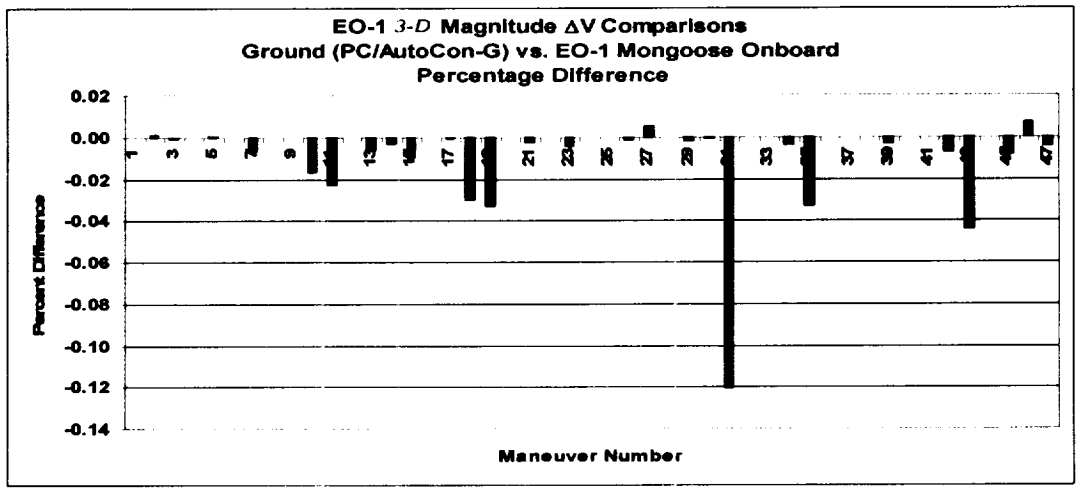

Figure 6. Percentage Difference in three-axis Onboard and Ground ΔVs

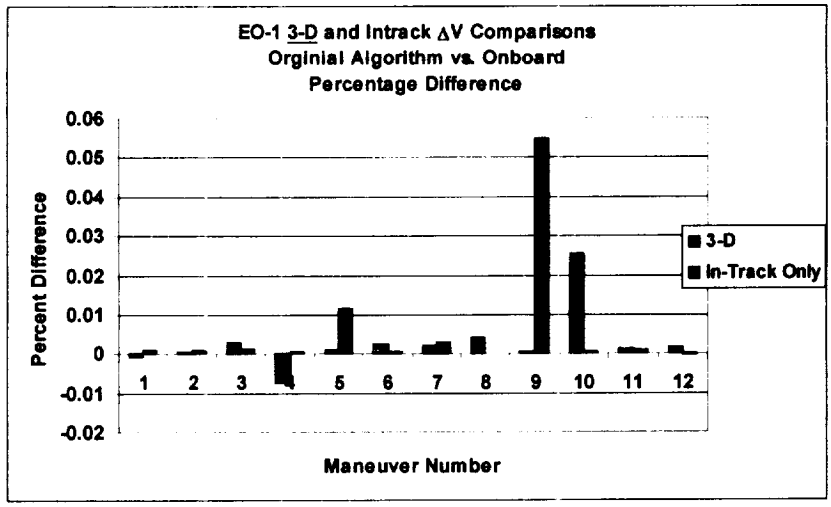

Figure 7. Percentage Difference in Original Algorithm and Onboard

Functional Propagation Comparisons

The FQ Algorithm is dependent upon the generation of the target and desired states. These states are propagated onboard using a Runge-Kutta 4/5 with an 8x8 Geopotential model and a Jacchia-Roberts atmospheric drag model. The accuracy of the computed ΔV is dependent upon the accuracy of these propagated states. For EO-1, the states are propagated forward 1½ orbits to compute the target state and then propagated 1½ orbits backward to compute the desired state. As the desired state incorporates the longest propagation duration with a restart, a comparison was made between the onboard and ground states. The comparison results are shown below in Figures 8 and 9. Figure 8 shows the position component and magnitude differences for six maneuver plans. Figure 9 shows the velocity differences. The maximum difference observed was 1.35 meters in the y-component of position and 1.4 cm/s in the z-component velocity. These small differences are still being investigated, but are believed to be the due to the RK4/5 integrator and performance of the EO-1 computer. The mean and standard deviations for position are listed in Table 1.

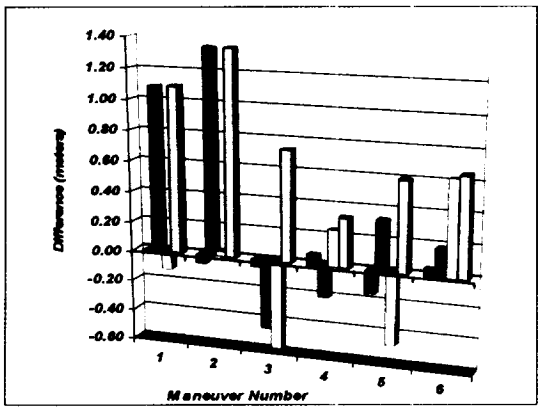

Figure 8. 1.5 Orbit Propagation Position Difference

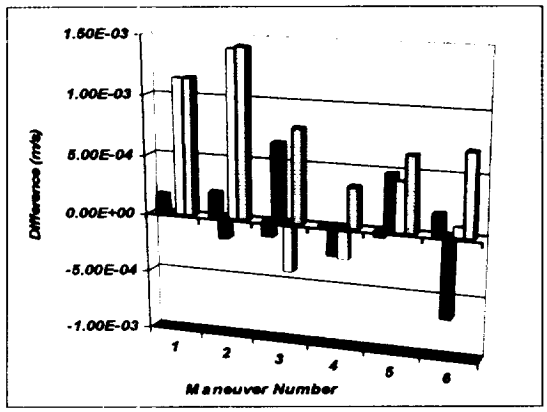

Figure 9. 1.5 Orbit Propagation Velocity Difference

Table 1
Propagation Mean and Standard Deviation for Desired State Computation

	X	Y	Z	Magnitude
Position Mean (m)	-0.02279	0.38221	-0.04550	0.79088
Position StDev (m)	0.07676	0.70684	0.45024	0.36886
Velocity Mean (m/s)	0.00007	0.00001	0.00040	0.00084
Velocity StDev (m/s)	0.00014	0.00049	0.00074	0.00039

Autonomous Maneuver Validation

A total of eight maneuvers were planned and validated in the manual, semi-autonomous, and fully autonomous mode. All were used to plan a formation flying maintenance maneuver with the semi-autonomous and autonomous mode generating commands onboard that were used onboard as well. The commands generated onboard in the fully autonomous mode were placed in the absolute time sequence with other spacecraft commands at approximately 12 hours before the maneuver execution. The locations and epochs of these maneuvers were chosen to meet the EO-1 orbit and science requirements in response to Landsat-7 maneuvers or to an EO-1 maneuver to maintain formation. The results presented in Tables 2 and 3 show that there is excellent agreement between the onboard system and the ground validation system. Tables 2 and 3 present

the maneuver mode and absolute ΔV difference and absolute percentage difference in the quantized and three-axis maneuvers. Table 2 gives results for the quantized maneuvers. Note that the percent error of the first ΔV computed from the Folta-Quinn algorithm (ΔV1) range from 0.000154% to 1.569%, the larger difference being the result of differences in the input target and desired states after propagation. The larger residual of the second velocity matching (ΔV2) is due to a 1-second quantization of a very small, 1.62 cm/s, 6 second long, velocity-matching maneuver. This difference is due to the onboard system yielding a maneuver duration near the mid-point which rounded down while the ground system rounded up. Table 3 provides the comparisons for the three-axis ΔVs required to align EO-1 directly behind Landsat-7 and involves all three ΔV components of radial, alongtrack, and crosstrack. The ΔVs for these maneuvers range from 10.8 m/s to a maximum of 15.6 m/s. Again, the comparisons are excellent with the range of percentage difference from the ground system at nearly zero to 0.66%. Additionally, a comparison was performed against the original algorithm with excellent results as the percentage differences were all under 0.005%.

Table 2
Quantized Maneuver Comparisons

Mode	Onboard ΔV1 cm/s	Onboard ΔV2 cm/s	Ground ΔV1 Difference cm/s	Ground ΔV2 Difference cm/s	% Diff ΔV1 vs. Ground %	% Diff ΔV2 vs. Ground %
Auto	4.9854078	0.0000000	0.0000001	0.0000000	0.00015645	0.00000000
Auto	2.4376271	3.7919202	0.0000003	0.0000002	0.00111324	0.00053176
Semi-Auto	1.0831335	1.6247106	0.0000063	-.0026969	0.05852198	-14.2361365
Semi-Auto	2.3841027	0.2649020	0.0000000	0.0000000	0.00011329	0.00073822
Semi-Auto	5.2980985	1.8543658	-0.0008450	-0.0002963	-1.56990117	-1.57294248
Manual	2.1915358	5.2049883	0.0000004	-0.0332099	0.00163366	-0.00022414
Manual	3.5555711	7.9318735	-0.0000003	-0.0272687	-0.00081327	3.57089537

Table 3
Three-Axis Maneuver Comparisons

Mode	Onboard ΔV1 m/s	Ground ΔV1 Difference cm/s	3-axis ΔV1 vs. Gnd %	Algorithm ΔV1 Diff cm/s	3-Axis ΔV1 vs. Alg %
Auto	10.8468	-0.0005441	-0.0000502	0.0003217	0.0000297
Auto	11.8633	0.0178726	0.0015066	-0.0101756	-0.0008577
Semi-Auto	12.6416	0.0311944	0.0024677	0.0091362	0.0002867
Semi-Auto	14.7610	0.1888158	0.0127932	0.0000000	0.0001196
Semi-Auto	15.3797	-0.2526237	-0.0164231	-0.0633549	-0.0045164
Manual	15.5790	10.4109426	0.6682668	-0.0117851	-0.0007565
Manual	15.4749	0.0018465	0.0001193	-0.0307683	-0.0021934

Maneuver Propagation Comparisons

As with the functional validation, a comparison of the propagated states used in computing the targeted and desired states is made. Figure 10 shows the comparisons of the inertial positions (x, y, and z) for the target and desired states. These states are computed using the same models as discussed in the functional validation. The largest difference can be seen in the columns marked

10-12. These differences occurred in the first semi-autonomous and last manual mode maneuvers. All the differences are less than 500 meters in all components with a standard deviation of less than 177 meters and less than 50 meters if the largest difference is excluded. Even so, these variations contributed to the differences between the onboard algorithm and the ground. The interval of propagation for these states is 13 hours for the manual maneuver modes and less than 2 hours for the semi-autonomous or fully autonomous mode.

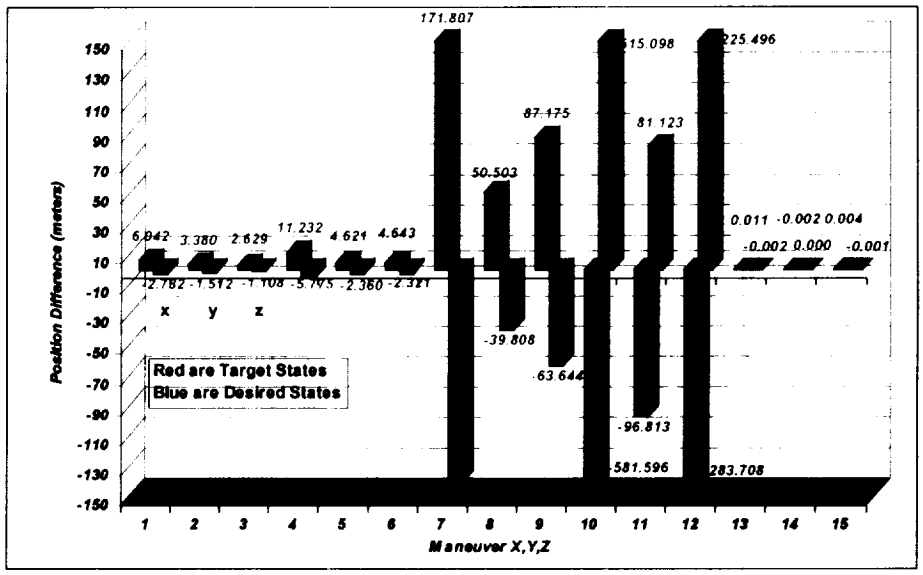

Figure 10. Target and Desired Propagation Position Differences

EO-1 Formation History of Relative Motion and Keplerian Orbit Parameters

The following relative motion and Keplerian parameter plots are taken from the definitive ephemeris of EO-1 and Landsat-7 orbit determination process as an independent check to verify that the formation requirements of 450km with a tolerance of 75km (+/- 42.5km yields 407.5km to 492.5km) and the ground track of +/-3km are met. Additionally, one can observe that the relative eccentricity and semi-major axis of the frozen orbit eccentricity were also maintained as a result of the formation flying maneuvers. Figure 11 shows the general formation flying evolution of the alongtrack and radial components presented in a Landsat-7 centered rotating coordinate system with the radial direction (ordinate) being the difference in radius magnitude and the alongtrack direction (abscissa) being the arc between the position vectors.

Figure 12 shows effect on the mission groundtrack by the formation flying maneuver and that it meets NMP requirements. The figure shows both EO-1 and Landsat-7 groundtracks as an offset from the world reference system grid. The time span is over the duration of the formation flying demonstration of 5 months from February 2001 to June 2001. At the beginning of the demonstration, EO-1 maneuvers only occurred in response to Landsat-7 maneuvers as the formation cycle were EO-1 exceeded the front of the control box was not completed before a Landsat-7 maneuver was required. Figure 13 shows the alongtrack separations over the demonstration duration. Figure 14 shows the semi-major axis evolution in which one can see the effects of the differential ballistic properties of each spacecraft. Figures 15 and 16 show the frozen orbit eccentricity and argument of periapsis. The data for these plots was generated

independently from the formation flying system and further show that the formation flying demonstration was a success.

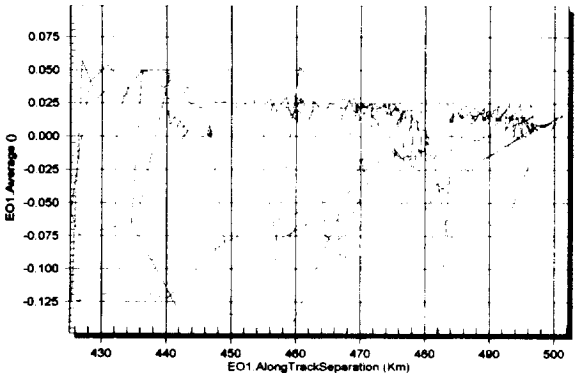

Figure 11 Radial vs. Alongtrack Distance

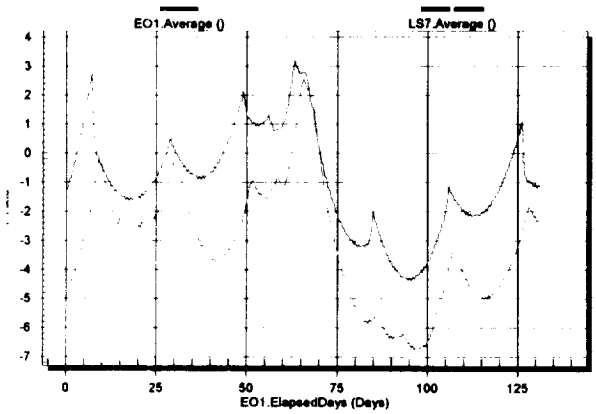

Figure 12 Groundtracks of EO-1(Green) and Landsat-7(Blue)

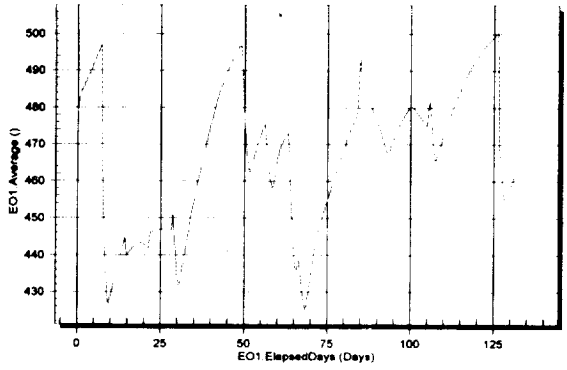

Figure 13 EO-1 Alongtrack Separation Evolution wrt Landsat-7

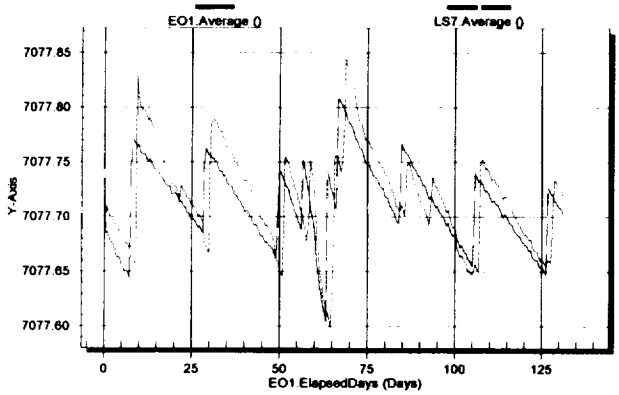

Figure 14 Sma Evolution of EO-1(Green) and Landsat-7(Blue)

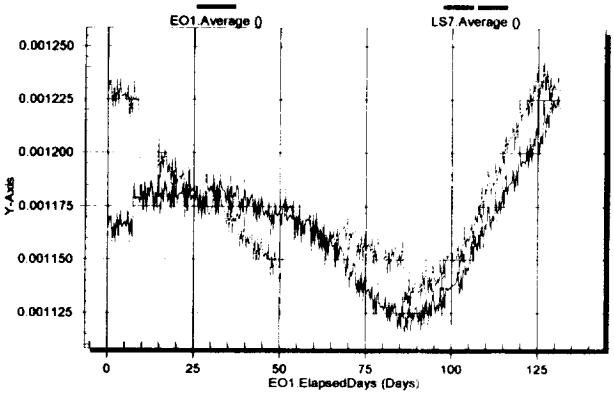

Figure 15 Eccentricity Evolution of EO-1(Green) and Landsat-7(Blue)

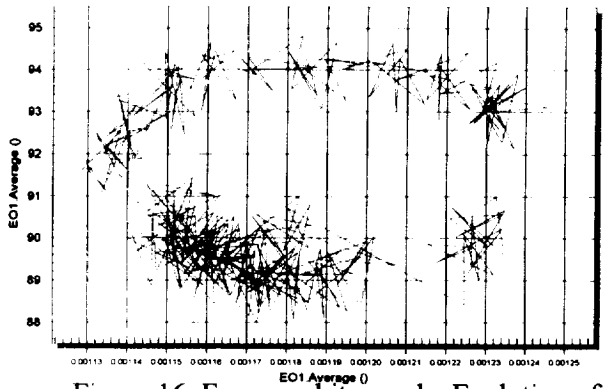

Figure 16 Frozen orbit ω and e Evolution of EO-1

SUMMARY

Using the formation flying algorithms developed by the Guidance, Navigation, and Control center of GSFC, onboard validation has shown that the EO-1 formation flying requirements can be easily met. To ensure the accuracy of the onboard FQ algorithm, several comparisons were performed against both original analytical calculations and ground based FQ numerical computations using AutoCon™ for given initial onboard-generated states. The FQ algorithm was validated by direct inputs of the initial states taken from the onboard system. The ΔV results agree to millimeters/sec level for the numerical tests which include the effects of propagation. This validation effort establishes the following:

- A demonstrated, validated fully non-linear autonomous system for formation flying.
- A precision algorithm for user defined control accuracy.
- A point-to-point formation flying algorithm using discretized maneuvers at user defined time intervals.
- A universal algorithm that incorporates.
    - intrack velocity changes for semimajor axis control,
    - radial changes for formation maintenance and eccentricity control
    - crosstrack changes for inclination control or node changes
    - any combination of the above for maintenance maneuvers
- Proven executive flight code.
- A system that incorporates fuzzy logic for multiple constraint checking for maneuver planning and control.
- Single or multiple maneuver computations.
- Multiple / generalized navigation inputs.
- Attitude (quaternion) required of the spacecraft to meet the ΔV components

CONCLUSIONS

The GSFC GNCC's Folta-Quinn formation flying algorithm is a innovative technology that can be used in a closed-loop design to meet science and mission requirements of all low Earth orbiting formation flying missions. The algorithm is very robust in that it supports not only benign groundtrack control and relative separation control, but also demanding three-axis control for inclination and non-Keplerian transfers. To best meet the NMP requirements, this innovative technology is flying onboard the EO-1 spacecraft. The algorithm was successfully integrated into AutoCon™ for ground support validation, closed-loop onboard autonomy, as well as operational support. The application of this algorithm and the AutoCon™ system to other NASA programs is unlimited, as it applies to any orbit about any planet and can be used to fully explore the NASA mandate of faster, better, cheaper spacecraft.

ACKNOWLEDGEMENT

The authors would like to thank the dedicated effort of Mr. Seth Shulman of Computer Sciences Corporation. As part of the EO-1 Flight Operations Team, Mr. Shulman was integral in maneuver planning and the technology validation process of the formation flying demonstration.

REFERENCES

1. F. Bauer, D. Quinn, K. Hartman, D. Folta, and J. Bristow "Enhanced Formation Flying Experiments For The New Millennium Program Earth Orbiter (EO)-1 Mission - Challenging Technology Program Management", AIAA, 5/97

2. J. Bristow, D. Folta, K. Hartman, and J. Leitner, "A Formation Flying Technology Vision", AIAA-2000-5194, February 2000

3. D. Folta and D. Quinn , "A Universal three-axis Method for Controlling the Relative Motion of Multiple Spacecraft in Any Orbit," Proceedings of the AIAA/AAS Astrodynamics Specialists Conference, August 10-12, Boston, MA.

4. D.Quinn and D. Folta (1996) *Patent Rights Application and Derivations of Autonomous Closed Loop 3-Axis Navigation Control Of EO-1.*

5. R. Battin, (1987) *An Introduction to the Mathematics and Methods of Astrodynamics*, AIAA Education Series, Chapters 9 and 11.

6 . R. Sperling, (1997) *AutoCon User's Guide Version 3.0, February 1998,* AI Solutions, Inc., Greenbelt, MD. 20770

7. D. Folta and A. Hawkins, " Preliminary Results of NASA's First Autonomous Formation Flying Experiement: Earth Observing-1 (EO-1), AIAA GSFC Flight Mechanics Symposium, Greenbelt Maryland, June 2001.

8. Matlab, The Math Works, Inc, Users Guide, 1995